

Observation of the Decay $\Lambda_b^0 \rightarrow \Lambda_c^+ \tau^- \bar{\nu}_\tau$

R. Aaij *et al.*^{*}
(LHCb Collaboration)



(Received 11 January 2022; accepted 29 March 2022; published 13 May 2022)

The first observation of the semileptonic b -baryon decay $\Lambda_b^0 \rightarrow \Lambda_c^+ \tau^- \bar{\nu}_\tau$, with a significance of 6.1σ , is reported using a data sample corresponding to 3 fb^{-1} of integrated luminosity, collected by the LHCb experiment at center-of-mass energies of 7 and 8 TeV at the LHC. The τ^- lepton is reconstructed in the hadronic decay to three charged pions. The ratio $\mathcal{K} = \mathcal{B}(\Lambda_b^0 \rightarrow \Lambda_c^+ \tau^- \bar{\nu}_\tau) / \mathcal{B}(\Lambda_b^0 \rightarrow \Lambda_c^+ \pi^- \pi^+ \pi^-)$ is measured to be $2.46 \pm 0.27 \pm 0.40$, where the first uncertainty is statistical and the second systematic. The branching fraction $\mathcal{B}(\Lambda_b^0 \rightarrow \Lambda_c^+ \tau^- \bar{\nu}_\tau) = (1.50 \pm 0.16 \pm 0.25 \pm 0.23)\%$ is obtained, where the third uncertainty is from the external branching fraction of the normalization channel $\Lambda_b^0 \rightarrow \Lambda_c^+ \pi^- \pi^+ \pi^-$. The ratio of semileptonic branching fractions $\mathcal{R}(\Lambda_c^+) \equiv \mathcal{B}(\Lambda_b^0 \rightarrow \Lambda_c^+ \tau^- \bar{\nu}_\tau) / \mathcal{B}(\Lambda_b^0 \rightarrow \Lambda_c^+ \mu^- \bar{\nu}_\mu)$ is derived to be $0.242 \pm 0.026 \pm 0.040 \pm 0.059$, where the external branching fraction uncertainty from the channel $\Lambda_b^0 \rightarrow \Lambda_c^+ \mu^- \bar{\nu}_\mu$ contributes to the last term. This result is in agreement with the standard model prediction.

DOI: 10.1103/PhysRevLett.128.191803

In the standard model of particle physics (SM) flavor-changing processes, such as semileptonic decays of b hadrons, are mediated by W^\pm bosons with universal coupling to leptons. Differences in the rates of decays involving the three lepton families are expected to arise only from the different masses of the charged leptons. Lepton flavour universality can be violated in many extensions of the SM with nonstandard flavor structure. Since the uncertainty due to hadronic effects cancels to a large extent, the SM predictions for the ratios between branching fractions of semileptonic decays of b hadrons, such as $\mathcal{R}(D^{(*)}) \equiv \mathcal{B}(\bar{B} \rightarrow D^{(*)} \tau^- \bar{\nu}_\tau) / \mathcal{B}(\bar{B} \rightarrow D^{(*)} \mu^- \bar{\nu}_\mu)$ [1–3], where $D^{(*)}$ and B mesons can be either charged or neutral, and $\mathcal{R}(\Lambda_c^+) \equiv \mathcal{B}(\Lambda_b^0 \rightarrow \Lambda_c^+ \tau^- \bar{\nu}_\tau) / \mathcal{B}(\Lambda_b^0 \rightarrow \Lambda_c^+ \mu^- \bar{\nu}_\mu)$, are known with uncertainties at the percent level [4–6]. These ratios therefore provide a sensitive probe of SM extensions [6,7].

Measurements of $\mathcal{R}(D^{0,+})$ and $\mathcal{R}(D^{*+,0})$ with τ^- decay final states involving electrons or muons have been reported by the *BABAR* [8,9] and *Belle* [10–12] Collaborations. The LHCb Collaboration published a determination of $\mathcal{R}(D^{*+})$ [13], where the τ lepton is reconstructed using leptonic decays to a muon. The LHCb experiment has also reported a measurement of $\mathcal{R}(D^{*+})$ using the three-prong decay $\tau^- \rightarrow \pi^- \pi^+ \pi^-(\pi^0) \nu_\tau$

[14]. These $\mathcal{R}(D^{(*),0})$ measurements yield values that are larger than the SM predictions with a combined significance of 3.4 standard deviations (σ) to date [15].

This Letter reports the observation of the decay $\Lambda_b^0 \rightarrow \Lambda_c^+ \tau^- \bar{\nu}_\tau$ and the first determination of $\mathcal{R}(\Lambda_c^+)$ using $\tau^- \rightarrow \pi^- \pi^+ \pi^-(\pi^0) \nu_\tau$ decays. The inclusion of charge-conjugate modes is implied throughout. The present work closely follows the strategy of Ref. [14]. Measurements in the baryonic sector provide complementary constraints on a potential lepton flavor universality violation because of the half-integer spin of the initial state [5,6]. The $\Lambda_b^0 \rightarrow \Lambda_c^+$ transition is determined by a different set of form factors with respect to the mesonic decays probed so far. Likewise, new physics couplings can also be different, resulting in different scenarios regarding deviations from SM expectations of $\mathcal{R}(\Lambda_c^+)$ and $\mathcal{R}(D^{(*)})$ [7].

A data sample of proton-proton (pp) collisions at center-of-mass energies $\sqrt{s} = 7$ and 8 TeV, corresponding to an integrated luminosity of 3 fb^{-1} , collected with the LHCb detector is used. The LHCb detector is a single-arm forward spectrometer covering the pseudorapidity range $2 < \eta < 5$, described in detail in Refs. [16,17]. The detector includes a high-precision tracking system consisting of a silicon-strip vertex detector surrounding the pp interaction region [18], and large-area silicon-strip detectors located upstream and downstream of the 4 Tm dipole magnet. The minimum distance of a track to a primary pp collision vertex (PV), the impact parameter (IP), is measured with a resolution of $(15 + 29/p_T) \mu\text{m}$, where p_T is the component of the momentum transverse to the beam direction, in GeV/c . The online event selection is performed by a trigger system [19], which consists of a hardware stage based on information from the calorimeter and muon systems, followed

^{*}Full author list given at the end of the article.

by a software stage that performs a full event reconstruction. Events are selected at the hardware stage if the particles forming the signal candidate satisfy a requirement on the energy deposited in the calorimeters or if any other particles pass any trigger algorithm. The software trigger requires a two-, three-, or four-track secondary vertex with significant displacement from any PV and consistent with the decay of a b hadron, or a three-track vertex with a significant displacement from any PV and consistent with the decay of a Λ_c^+ baryon. A multivariate algorithm is used for the identification of secondary vertices consistent with the decay of a b hadron, while secondary vertices consistent with the decay of a Λ_c^+ baryon are identified using topological criteria. In the simulation, pp collisions are generated using PYTHIA8 [20] with a specific LHCb configuration [21]. Decays of hadronic particles are described by EVTGEN [22], in which final-state radiation is generated using PHOTOS [23]. The TAUOLA package [24] is used to simulate the decays of the τ^- lepton into $3\pi\nu_\tau$ and $3\pi\pi^0\nu_\tau$ final states, where $3\pi \equiv \pi^-\pi^+\pi^-$, according to the resonance chiral Lagrangian model [25] with a tuning based on the results from the BABAR Collaboration [26]. The interaction of the generated particles with the detector, and its response, are implemented using the GEANT4 toolkit [27] as described in Ref. [28]. The signal decays are simulated using form factors that are derived from heavy-quark effective theory [29].

The Λ_c^+ baryon candidates are reconstructed using the $\Lambda_c^+ \rightarrow pK^-\pi^+$ decay mode, by combining three charged tracks compatible with proton, kaon, and pion hypotheses. The τ^- candidates are formed by $\pi^-\pi^+\pi^-$ combinations and include contributions from the $\tau^- \rightarrow 3\pi\nu_\tau$ and $\tau^- \rightarrow 3\pi\pi^0\nu_\tau$ decay modes, as neutral pions are not reconstructed. The Λ_c^+ and τ^- candidates are selected based on kinematic, geometric, and particle-identification criteria. The Λ_b^0 candidate is formed by combining a Λ_c^+ and a τ^- candidate. Background due to misreconstructed b hadrons, where at least one additional particle originates from either the 3π vertex or the b -hadron vertex, is suppressed by requiring a single Λ_b^0 candidate per event. Tracks other than those used for the signal candidate are exploited in a multivariate algorithm to assess the signal isolation, i.e., the absence of extra tracks compatible with the 3π vertex [30]. The algorithm is trained on simulated samples of $\Lambda_b^0 \rightarrow \Lambda_c^+\tau^-\bar{\nu}_\tau$ and $\Lambda_b^0 \rightarrow \Lambda_c^+\bar{D}^0K^-$ decays for signal and background, respectively; its efficiency is 20% higher than the cut-based algorithm used in Ref. [14] for the same rejection factor. Likewise, the neutral-particle energy contained in a cone centred around the direction of the τ^- candidates is used to further separate signal and background processes. The τ^- momentum can be determined, up to a twofold ambiguity, from the momentum vector of the 3π system and the flight direction of the τ^- candidate. The average of the two solutions is used, as discussed in Ref. [14]. The same

method is used to compute the Λ_b^0 momentum. This enables the computation of the invariant mass squared of the $\tau^-\bar{\nu}_\tau$ lepton pair (q^2), and the pseudo decay time of the τ^- candidate (t_τ). The variables q^2 and t_τ are reconstructed with a resolution of roughly 15%, providing good discrimination between the signal and background processes.

The finite τ^- lifetime causes the 3π vertex to be detached from the Λ_b^0 vertex. This key feature allows the suppression of the large background, called prompt background hereafter, from b hadrons decaying to a Λ_c^+ baryon accompanied by a 3π system being produced promptly at the b -hadron decay vertex, plus any other unreconstructed particles (X). The difference of the positions of the 3π and the Λ_c^+ vertices along the beam direction is required to be at least 5 times larger than its uncertainty. This requirement suppresses the prompt background 10 times more than the selection used in Ref. [14], reducing this initially dominant background to a negligible level, at a price of 50% reduction of the signal efficiency.

Double-charm background processes due to Λ_b^0 baryon decays into a Λ_c^+ baryon plus another charmed hadron that subsequently decays into a final state containing three charged pions, are topologically similar to the signal and constitute the largest background source. The main contribution originates from $\Lambda_b^0 \rightarrow \Lambda_c^+D_s^-(X)$ decays, with D_s^- decays to $3\pi Y$ final states, where Y stands for any set of extra particles, such as one or two π^0 mesons. Such D_s^- decays have a large branching fraction (~30%) [31]. This background is reduced principally by taking into account the resonant structure of the 3π system. The $\tau^- \rightarrow 3\pi\nu_\tau$ decays proceed predominantly through the $a_1(1260)^- \rightarrow \rho^0\pi^-$ decay. By contrast, the $D_s^- \rightarrow 3\pi Y$ decays occur mainly through the η and η' resonances. This feature, captured by the shapes of the distributions of the smaller and larger mass of the two $\pi^+\pi^-$ combinations extracted from each 3π candidate, the energy carried by neutral particles within the cone around the 3π direction, and kinematic variables from partial reconstruction are exploited by means of a boosted decision tree (BDT) classifier [32,33], as described in Ref. [14]. Figure 4 of the Supplemental Material [34] displays the markedly different distributions of the three main input variables to the BDT classifier obtained for signal and D_s^- background, respectively. The partial reconstruction of the Λ_b^0 decay kinematics is performed under the background hypothesis where the Λ_b^0 particle decays to $\Lambda_c^+D_s^-(\rightarrow 3\pi Y)$. The BDT response in simulation is validated using three control samples: the $\Lambda_b^0 \rightarrow \Lambda_c^+3\pi$ normalization sample; a $\Lambda_b^0 \rightarrow \Lambda_c^+\bar{D}^0(X)$ data sample with the subsequent $\bar{D}^0 \rightarrow K^+3\pi$ decay, which is obtained by removing the charged-particle isolation criterion and requiring an additional charged kaon originating from the 3π vertex; and a $\Lambda_b^0 \rightarrow \Lambda_c^+D^-(X)$ data sample, using $D^- \rightarrow K^+\pi^-\pi^-$ decays, which is obtained by assigning a kaon mass to the

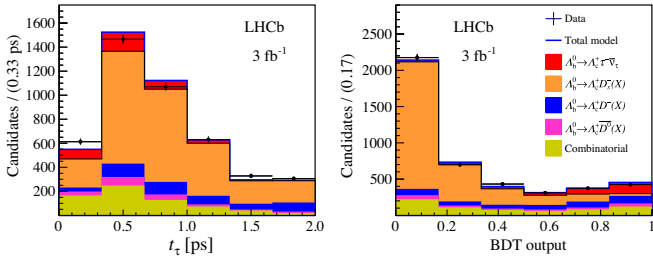


FIG. 1. Distributions of (left) τ^- decay time and (right) BDT output for $\Lambda_b^0 \rightarrow \Lambda_c^+ \tau^- \bar{\nu}_\tau$ candidates. Projections of the three-dimensional fit results are overlaid. The various fit components are described in the legend.

positively charged pion of the τ^- candidate. For all these samples, good agreement between data and simulation is observed in the distributions of the variables used in the BDT classifier.

The signal yield is measured using a three-dimensional binned maximum-likelihood fit to t_τ , the BDT output, and q^2 , which are shown in Fig. 1 and 2. The fit model includes a signal component; background components due to $B \rightarrow \Lambda_c^+ D_s^-(X)$, $\Lambda_b^0 \rightarrow \Lambda_c^+ D^-(X)$, and $\Lambda_b^0 \rightarrow \Lambda_c^+ \bar{D}^0(X)$ decays; background due to misreconstructed Λ_c^+ candidates; and combinatorial background. Template distributions for signal and background are obtained from simulation, with the exceptions of random $pK^-\pi^+$ combinations and the combinatorial background, which are constructed from data-based control samples. The signal template accounts for both $\tau^- \rightarrow 3\nu_\tau$ and $\tau^- \rightarrow 3\pi\pi^0\nu_\tau$ decays, where the fraction of the former is fixed to 78% according to the branching fractions and selection efficiencies. A contribution from $\Lambda_b^0 \rightarrow \Lambda_c^{*+} \tau^- \bar{\nu}_\tau$ decays, where Λ_c^{*+} denotes any excited charmed baryon state decaying into final states involving Λ_c^+ baryon, constitutes a feed down to the signal. Its yield fraction is constrained to be $(10 \pm 5)\%$ of the signal yield, derived from the Λ_c^{*+} relative abundance as measured in the $\Lambda_b^0 \rightarrow \Lambda_c^{*+} \pi^- \pi^+ \pi^-$ decays, their respective branching fractions in the $\Lambda_c^+ \pi^0 \pi^0$ and $\Lambda_c^+ \pi^+ \pi^-$ modes [31], and the corresponding selection efficiency obtained from simulation. The background

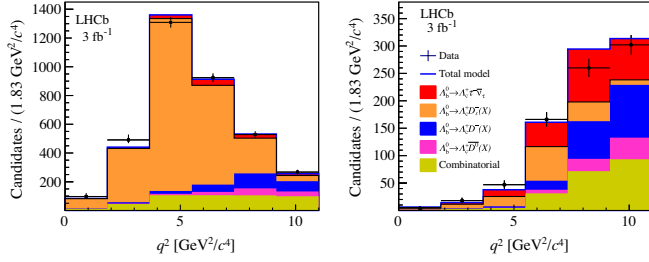


FIG. 2. Distributions of q^2 for $\Lambda_b^0 \rightarrow \Lambda_c^+ \tau^- \bar{\nu}_\tau$ candidates having a BDT output value (left) below and (right) above 0.66. Projections of the three-dimensional fit are overlaid. The various fit components are described in the legend.

originating from decays of $\Lambda_b^0 \rightarrow \Lambda_c^+ D_s^-(X)$ is divided into contributions from $\Lambda_b^0 \rightarrow \Lambda_c^+ D_s^-$, $\Lambda_b^0 \rightarrow \Lambda_c^+ D_s^{*-}$, $\Lambda_b^0 \rightarrow \Lambda_c^+ D_{s0}^*(2317)^-$, $\Lambda_b^0 \rightarrow \Lambda_c^+ D_{s1}(2460)^-$, and $\Lambda_b^0 \rightarrow \Lambda_c^{*+} D_s^-(X)$ decays. A control sample of $\Lambda_b^0 \rightarrow \Lambda_c^+ 3\pi$ candidates, where the 3π invariant mass is selected within 45 MeV/ c^2 of the known D_s^- mass [31] is shown in Fig. 3. The relative yield of each of the above-mentioned background processes is constrained using the results of a fit to the $\Lambda_c^+ \pi^- \pi^+ \pi^-$ mass distribution.

The D_s^- decay model used in the simulation does not accurately describe the data because of the limited knowledge of the D_s^- decay amplitudes to $3\pi Y$ final states. A correcting factor, taken from high precision $\bar{B}^0 \rightarrow D^{*+} D_s^-$ sample [14], is applied to each D_s^- branching fraction to match the $\pi^- \pi^+ \pi^-$ Dalitz distributions from simulation to those observed in data.

The background originating from $\Lambda_b^0 \rightarrow \Lambda_c^+ \bar{D}^0(X)$ decays is subdivided into two contributions, depending on whether the 3π system originates from the \bar{D}^0 vertex, or whether one pion originates from the \bar{D}^0 vertex and the other two from elsewhere. The former contribution is constrained by the yield obtained from the $\Lambda_b^0 \rightarrow \Lambda_c^+ \bar{D}^0(X)$ control sample. The template associated to $\Lambda_c^+ \bar{D}^0(X)$ background is also validated using the data-driven sample where the $\bar{D}^0 \rightarrow K^+ 3\pi$ decay is fully reconstructed. The yield of the other $\Lambda_b^0 \rightarrow \Lambda_c^+ \bar{D}^0(X)$ background component is a free parameter in the fit. The yield of the $\Lambda_b^0 \rightarrow \Lambda_c^+ D^-(X)$ background is also a free parameter and its template is validated using the data-driven sample with the D^- meson fully reconstructed in the $K^+ \pi^- \pi^-$ mode.

The combinatorial background is divided into two contributions, depending on whether the Λ_b^0 candidate contains a true Λ_c^+ baryon or a random $pK^-\pi^+$ combination. In the first case, the Λ_c^+ and the 3π system originate

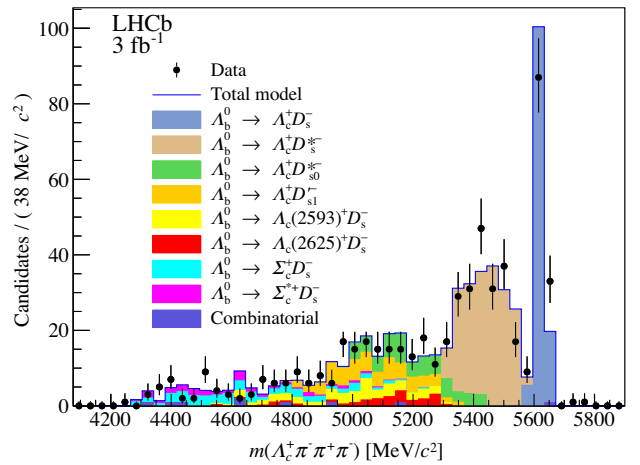


FIG. 3. Distribution of the $\Lambda_c^+ \pi^- \pi^+ \pi^-$ invariant mass for the $\Lambda_b^0 \rightarrow \Lambda_c^+ D_s^-(X)$ control sample, with $D_s^- \rightarrow \pi^- \pi^+ \pi^-$. The components contributing to the fit model are indicated in the legend.

from different b -hadron decays. The data sample of wrong-sign Λ_b^0 candidates where the Λ_c^+ and the 3π system have the same electric charge is used to obtain a background template. Its yield is obtained by normalizing to the right-sign data in the region where the reconstructed $\Lambda_c^+3\pi$ mass is significantly larger than the known Λ_b^0 mass [14]. The background not including a true Λ_c^+ baryon is parametrized using a specific data sample originating from Λ_b^0 candidates where the Λ_c^+ candidate has a mass outside a window of $15 \text{ MeV}/c^2$ around the known Λ_c^+ mass [31].

The projections of the fit on t_τ and the BDT output are shown in Fig. 1. The projections on q^2 in two different BDT output ranges are shown in Fig. 2. The signal yield is $N_{\text{sig}} = 349 \pm 40$. The fit is repeated with all nuisance parameters related to the template shapes varying freely, while the signal yield is fixed at zero. The χ^2 variation derived from the change of the fit maximum likelihood corresponds to an increase of 6.1σ with respect to the default fit with freely varying signal yield. This measurement signifies the first observation of the decay $\Lambda_b^0 \rightarrow \Lambda_c^+ \tau^- \bar{\nu}_\tau$. A clear separation between signal and the main background originating from $\Lambda_b^0 \rightarrow \Lambda_c^+ D_s^+(X)$ decays is obtained, as demonstrated in the BDT distribution of Fig. 1. Figure 2 shows that the $\Lambda_b^0 \rightarrow \Lambda_c^+ D_s^+(X)$ background is dominant at low BDT values, while a good signal-to-background ratio is observed at high BDT output. Figure 5 of the Supplemental Material [34] shows similarly the τ decay time distribution for the same BDT intervals.

In order to reduce experimental systematic uncertainties, the $\Lambda_b^0 \rightarrow \Lambda_c^+ 3\pi$ decay is chosen as a normalization channel. This leads to a measurement of the ratio

$$\mathcal{K}(\Lambda_c^+) \equiv \frac{\mathcal{B}(\Lambda_b^0 \rightarrow \Lambda_c^+ \tau^- \bar{\nu}_\tau)}{\mathcal{B}(\Lambda_b^0 \rightarrow \Lambda_c^+ 3\pi)} = \frac{N_{\text{sig}} \epsilon_{\text{norm}}}{N_{\text{norm}} \epsilon_{\text{sig}}} \frac{1}{\mathcal{B}(\tau^- \rightarrow 3\pi(\pi^0)\nu_\tau)}, \quad (1)$$

where N_{sig} (N_{norm}) and ϵ_{sig} (ϵ_{norm}) are the yield and selection efficiency for the signal (normalisation) channel, respectively. The normalization channel selection is identical to that of the signal channel, except the requirement that the 3π system has a larger flight distance than that of the Λ_c^+ candidate, which is not imposed. The yield of the normalization mode is determined by fitting the invariant-mass distribution of the $\Lambda_c^+ 3\pi$ candidates around the known Λ_b^0 mass [31], as shown in Fig. 6 of Supplemental Material [34]. A significant contribution from excited baryons which decay to $\Lambda_c^+ \pi^+ \pi^-$, $\Lambda_c^+ \pi^+$, or $\Lambda_c^+ \pi^-$ is explicitly vetoed from the normalization channel. As a result, the 3π dynamics resembles that of the signal, leading to a reduced systematic uncertainty.

A normalization yield of $N_{\text{norm}} = 8584 \pm 102$ is found, after subtraction of a small contribution of 168 ± 20 $\Lambda_b^0 \rightarrow \Lambda_c^+ D_s^- (\rightarrow 3\pi)$ decays. This component is estimated by

fitting the 3π mass distribution in the D_s^- mass region for candidates with a reconstructed $\Lambda_c^+ 3\pi$ mass in a window around the known Λ_b^0 mass [31]. The normalization sample is also used to correct for differences in the Λ_b^0 production kinematics between data and simulation. The reconstruction efficiencies for the $\tau^- \rightarrow 3\pi\nu_\tau$, $\tau^- \rightarrow 3\pi\pi^0\nu_\tau$ signal modes and normalization channel are determined using the simulation and found to be $(1.37 \pm 0.04) \times 10^{-5}$, $(0.82 \pm 0.05) \times 10^{-5}$, and $(11.21 \pm 0.11) \times 10^{-5}$, respectively. The ratio of branching fractions is derived from Eq. (1) as

$$\mathcal{R}(\Lambda_c^+) = 2.46 \pm 0.27 \pm 0.40,$$

where the first uncertainty is statistical and the second systematic.

Using $\mathcal{B}(\Lambda_b^0 \rightarrow \Lambda_c^+ 3\pi) = (6.14 \pm 0.94) \times 10^{-3}$ [31] corresponding to an average of measurements by the CDF [35] and LHCb [36] experiments, the signal branching fraction is determined as

$$\mathcal{B}(\Lambda_b^0 \rightarrow \Lambda_c^+ \tau^- \bar{\nu}_\tau) = (1.50 \pm 0.16 \pm 0.25 \pm 0.23)\%,$$

where the first uncertainty is statistical, the second systematic, and the third is due to the external branching fraction measurement. The branching fraction $\mathcal{B}(\Lambda_b^0 \rightarrow \Lambda_c^+ \mu^- \bar{\nu}_\mu) = (6.2 \pm 1.4)\%$ from the DELPHI experiment [37] updated in Ref. [31] is used to obtain the ratio of semileptonic branching fractions $\mathcal{R}(\Lambda_c^+)$ as

$$\mathcal{R}(\Lambda_c^+) = 0.242 \pm 0.026 \pm 0.040 \pm 0.059,$$

where the first uncertainty is statistical, the second systematic, and the third is due to the external branching fractions measurements. The measured value of $\mathcal{R}(\Lambda_c^+)$ is lower than, but in agreement with, the standard model prediction of 0.324 ± 0.004 [5].

The sources of systematic uncertainty of $\mathcal{K}(\Lambda_c^+)$ are reported in Table I. For $\mathcal{B}(\Lambda_b^0 \rightarrow \Lambda_c^+ \tau^- \bar{\nu}_\tau)$ and $\mathcal{R}(\Lambda_c^+)$, the systematic uncertainties related to the external branching fractions are added in quadrature. The uncertainty due to the limited size of the simulated samples is computed by repeatedly sampling each template with a bootstrap procedure, performing the fit, and taking the standard deviation of the resulting spread of N_{sig} values. The limited size of the simulated samples also contributes to the systematic uncertainty in the efficiencies for signal and normalisation modes. The systematic uncertainty associated with the signal decay model originates from the limited knowledge of the form factors and the τ^- polarization. The form factor distributions are varied in their range allowed by measurements from $\Lambda_b^0 \rightarrow \Lambda_c^+ \mu^- \bar{\nu}_\mu$ decays. The contribution from the relative branching fractions and selection efficiencies of $\tau^- \rightarrow 3\pi\pi^0\nu_\tau$ and

TABLE I. Relative systematic uncertainties in $\mathcal{K}(\Lambda_c^+)$.

Source	$\delta\mathcal{K}(\Lambda_c^+)/\mathcal{K}(\Lambda_c^+) (\%)$
Simulated sample size	3.8
Fit bias	3.9
Signal modeling	2.0
$\Lambda_b^0 \rightarrow \Lambda_c^{*+} \tau^- \bar{\nu}_\tau$ feed down	2.5
$D_s^- \rightarrow 3\pi Y$ decay model	2.5
$\Lambda_b^0 \rightarrow \Lambda_c^+ D_s^- X$, $\Lambda_b^0 \rightarrow \Lambda_c^+ D^- X$, $\Lambda_b^0 \rightarrow \Lambda_c^+ \bar{D}^0 X$ background	4.7
Combinatorial background	0.5
Particle identification and trigger corrections	1.5
Isolation BDT classifier and vertex selection requirements	4.5
D_s^-, D^-, \bar{D}^0 template shapes	13.0
Efficiency ratio	2.8
Normalization channel efficiency (modeling of $\Lambda_b^0 \rightarrow \Lambda_c^+ 3\pi$)	3.0
Total uncertainty	16.5

$\tau^- \rightarrow 3\pi\nu_\tau$ decays are computed by varying their ratio within their uncertainties. Potential contribution from other τ^- decay modes is investigated through a dedicated simulation including all known τ^- decay modes. The feed-down contribution where the τ^- is produced in association with an excited charmed baryon is computed varying in the fit the relative amount of such decays in their allowed range of $(10 \pm 5)\%$. The uncertainty due to the knowledge of the D_s^- decay model is estimated by repeatedly varying the correction factors of the templates within their uncertainties, as determined from the associated control sample, and performing the fit. The spread of the fit results is assigned as the corresponding systematic uncertainty.

The template shapes of the $\Lambda_b^0 \rightarrow \Lambda_c^+ D_s^-(X)$, $\Lambda_b^0 \rightarrow \Lambda_c^+ \bar{D}^0 X$, and $\Lambda_b^0 \rightarrow \Lambda_c^+ D^-(X)$ background modes depend on the dynamics of the corresponding decays. A range of template deformations [14] is performed, and the spread of the fit results is taken as a systematic uncertainty. The resulting uncertainty of 13% represents the largest single source. A similar procedure is applied to the template for the combinatorial background. The contribution from a potential bias in the fit is explored by fitting pseudoexperiments where the signal strength is varied from its SM value to a negligible amount. Other sources of systematic uncertainty arise from the inaccuracy on the yields of the various background contributions, and from the limited knowledge of the normalization channel modeling. The contribution from the removal of Λ_c^{*+} modes from the normalization channel is taken into account by varying the branching fractions of the various excited baryon decays within their measured range.

Systematic effects in the efficiencies for signal and normalization channels partially cancel in the ratio, with the remaining uncertainty being mostly due to the limited

size of the simulated sample. The trigger efficiency depends on the distributions of the decay time of the τ^- candidates and the invariant mass of the $\Lambda_c^+ 3\pi$ system. These distributions differ between the signal and normalization modes, and the corresponding difference of the trigger efficiencies is taken into account.

In conclusion, the first observation of the semileptonic decay $\Lambda_b^0 \rightarrow \Lambda_c^+ \tau^- \bar{\nu}_\tau$ is reported with a significance of 6.1σ , using a data sample of pp collisions, corresponding to 3 fb^{-1} of integrated luminosity, collected by the LHCb experiment. The measurement exploits the three-prong hadronic τ^- decays with the technique pioneered by the LHCb experiment for the $\mathcal{R}(D^{*+})$ measurement [14]. The ratio $\mathcal{K} = \mathcal{B}(\Lambda_b^0 \rightarrow \Lambda_c^+ \tau^- \bar{\nu}_\tau)/\mathcal{B}(\Lambda_b^0 \rightarrow \Lambda_c^+ \pi^- \pi^+ \pi^-)$ is measured to be $2.46 \pm 0.27 \pm 0.40$, where the first uncertainty is statistical and the second systematic. The branching fraction $\mathcal{B}(\Lambda_b^0 \rightarrow \Lambda_c^+ \tau^- \bar{\nu}_\tau)$ is measured to be $(1.50 \pm 0.16 \pm 0.25 \pm 0.23)\%$, where the third uncertainty is due to external branching fraction measurements. A measurement of $\mathcal{R}(\Lambda_c^+) = 0.242 \pm 0.026 \pm 0.040 \pm 0.059$ is reported. The $\mathcal{R}(\Lambda_c^+)$ ratio is found to be in agreement with the SM prediction. This measurement provides constraints on new physics models, such as some of those described in Ref. [6], for which large values of $\mathcal{R}(\Lambda_c^+)$ are allowed by existing $\mathcal{R}(D^{(*)})$ measurements.

We express our gratitude to our colleagues in the CERN accelerator departments for the excellent performance of the LHC. We thank the technical and administrative staff at the LHCb institutes. We acknowledge support from CERN and from the national agencies: CAPES, CNPq, FAPERJ and FINEP (Brazil); MOST and NSFC (China); CNRS/IN2P3 (France); BMBF, DFG and MPG (Germany); INFN (Italy); NWO (Netherlands); MNiSW and NCN (Poland); MEN/IFA (Romania); MSHE (Russia); MICINN (Spain); SNSF and SER (Switzerland); NASU (Ukraine); STFC (United Kingdom); DOE NP and NSF (USA). We acknowledge the computing resources that are provided by CERN, IN2P3 (France), KIT and DESY (Germany), INFN (Italy), SURF (Netherlands), PIC (Spain), GridPP (United Kingdom), RRCKI and Yandex LLC (Russia), CSCS (Switzerland), IFIN-HH (Romania), CBPF (Brazil), PL-GRID (Poland), and NERSC (USA). We are indebted to the communities behind the multiple open-source software packages on which we depend. Individual groups or members have received support from ARC and ARDC (Australia); AvH Foundation (Germany); EPLANET, Marie Skłodowska-Curie Actions and ERC (European Union); A*MIDEX, ANR, IPhU, and Labex P2IO, and Région Auvergne-Rhône-Alpes (France); Key Research Program of Frontier Sciences of CAS, CAS PIFI, CAS CCEPP, Fundamental Research Funds for the Central Universities, and Sci. & Tech. Program of Guangzhou (China); RFBR, RSF, and Yandex LLC (Russia); GVA, XuntaGal, and GENCAT (Spain); the Leverhulme Trust, the Royal Society, and UKRI (United Kingdom).

- [1] D. Bigi and P. Gambino, Revisiting $B \rightarrow D\ell\nu$, *Phys. Rev. D* **94**, 094008 (2016).
- [2] S. Jaiswal, S. Nandi, and S. K. Patra, Updates on extraction of $|V_{cb}|$ and SM prediction of $R(D^*)$ in $B \rightarrow D^*\ell\nu_\ell$ decays, *J. High Energy Phys.* **06** (2020) 165.
- [3] F. U. Bernlochner, Z. Ligeti, M. Papucci, and D. J. Robinson, Combined analysis of semileptonic B decays to D and D^* : $R(D^{(*)})$, $|V_{cb}|$, and new physics, *Phys. Rev. D* **95**, 115008 (2017); **97**, 059902(E) (2018).
- [4] F. U. Bernlochner, Z. Ligeti, D. J. Robinson, and W. L. Sutcliffe, $\Lambda_b \rightarrow \Lambda_c$ Semileptonic Decays and Tests of Heavy Quark Symmetry, *Phys. Rev. Lett.* **121**, 202001 (2018).
- [5] F. U. Bernlochner, Z. Ligeti, D. J. Robinson, and W. L. Sutcliffe, Precise predictions for $\Lambda_b \rightarrow \Lambda_c$ semileptonic decays, *Phys. Rev. D* **99**, 055008 (2019).
- [6] A. Datta, S. Kamali, S. Meinel, and A. Rashed, Phenomenology of $\Lambda_b \rightarrow \Lambda_c \tau \bar{\nu}_\tau$ using lattice QCD calculations, *J. High Energy Phys.* **08** (2017) 131.
- [7] F. U. Bernlochner, M. F. Sevilla, D. J. Robinson, and G. Wormser, Semitauonic b -hadron decays: A lepton flavor universality laboratory, *Rev. Mod. Phys.* **94**, 015003 (2022).
- [8] J. P. Lees *et al.* (BABAR Collaboration), Evidence for an Excess of $\bar{B} \rightarrow D^{(*)}\tau^-\bar{\nu}_\tau$ Decays, *Phys. Rev. Lett.* **109**, 101802 (2012).
- [9] J. P. Lees *et al.* (BABAR Collaboration), Measurement of an excess of $\bar{B} \rightarrow D^{(*)}\tau^-\bar{\nu}_\tau$ decays and implications for charged Higgs bosons, *Phys. Rev. D* **88**, 072012 (2013).
- [10] M. Huschle *et al.* (Belle Collaboration), Measurement of the branching ratio of $\bar{B} \rightarrow D^{(*)}\tau^-\bar{\nu}_\tau$ relative to $\bar{B} \rightarrow D^{(*)}\ell^-\bar{\nu}_\ell$ decays with hadronic tagging at Belle, *Phys. Rev. D* **92**, 072014 (2015).
- [11] G. Caria *et al.* (Belle Collaboration), Measurement of $\mathcal{R}(D)$ and $\mathcal{R}(D^*)$ with a Semileptonic Tagging Method, *Phys. Rev. Lett.* **124**, 161803 (2020).
- [12] S. Hirose *et al.* (Belle Collaboration), Measurement of the τ lepton polarization and $R(D^*)$ in the decay $\bar{B} \rightarrow D^*\tau^-\bar{\nu}_\tau$ with one-prong hadronic τ decays at Belle, *Phys. Rev. D* **97**, 012004 (2018).
- [13] R. Aaij *et al.* (LHCb Collaboration), Measurement of the ratio of branching fractions $\mathcal{B}(\bar{B}^0 \rightarrow D^{*+}\tau^-\bar{\nu}_\tau)/\mathcal{B}(\bar{B}^0 \rightarrow D^{*+}\mu^-\bar{\nu}_\mu)$, *Phys. Rev. Lett.* **115**, 111803 (2015); **115**, 159901 (2015).
- [14] R. Aaij *et al.* (LHCb Collaboration), Test of lepton flavor universality by the measurement of the $B^0 \rightarrow D^{*-}\tau^+\nu_\tau$ branching fraction using three-prong τ decays, *Phys. Rev. D* **97**, 072013 (2018).
- [15] Y. Amhis *et al.* (Heavy Flavor Averaging Group), Averages of b -hadron, c -hadron, and τ -lepton properties as of 2018, *Eur. Phys. J. C* **81**, 226 (2021).
- [16] A. A. Alves Jr. *et al.* (LHCb Collaboration), The LHCb detector at the LHC, *J. Instrum.* **3**, S08005 (2008).
- [17] R. Aaij *et al.* (LHCb Collaboration), LHCb detector performance, *Int. J. Mod. Phys. A* **30**, 1530022 (2015).
- [18] R. Aaij *et al.*, Performance of the LHCb vertex locator, *J. Instrum.* **9**, P09007 (2014).
- [19] R. Aaij *et al.*, The LHCb trigger and its performance in 2011, *J. Instrum.* **8**, P04022 (2013).
- [20] T. Sjöstrand, S. Mrenna, and P. Skands, PYTHIA6.4 physics and manual, *J. High Energy Phys.* **05** (2006) 026; A brief introduction to PYTHIA8.1, *Comput. Phys. Commun.* **178**, 852 (2008).
- [21] I. Belyaev *et al.*, Handling of the generation of primary events in Gauss, the LHCb simulation framework, *J. Phys. Conf. Ser.* **331**, 032047 (2011).
- [22] D. J. Lange, The EvtGen particle decay simulation package, *Nucl. Instrum. Methods Phys. Res., Sect. A* **462**, 152 (2001).
- [23] N. Davidson, T. Przedzinski, and Z. Was, PHOTOS interface in C++: Technical and physics documentation, *Comput. Phys. Commun.* **199**, 86 (2016).
- [24] N. Davidson, G. Nanava, T. Przedziński, E. Richter-Was, and Z. Was, Universal interface of TAUOLA technical and physics documentation, *Comput. Phys. Commun.* **183**, 821 (2012).
- [25] I. M. Nugent, T. Przedziński, P. Roig, O. Shekhovtsova, and Z. Was, Resonance chiral Lagrangian currents and experimental data for $\tau^- \rightarrow \pi^-\pi^-\pi^+\nu_\tau$, *Phys. Rev. D* **88**, 093012 (2013).
- [26] I. M. Nugent, T. Przedzinski, P. Roig, O. Shekhovtsova, and Z. Was, Invariant mass spectra of $\tau^- \rightarrow h^-h^-h^+\nu_\tau$ decays, *Nucl. Phys. B, Proc. Suppl.* **253–255**, 38 (2014).
- [27] J. Allison *et al.* (Geant4 Collaboration), Geant4 developments and applications, *IEEE Trans. Nucl. Sci.* **53**, 270 (2006); S. Agostinelli *et al.* (Geant4 Collaboration), Geant4: A simulation toolkit, *Nucl. Instrum. Methods Phys. Res., Sect. A* **506**, 250 (2003).
- [28] M. Clemencic, G. Corti, S. Easo, C. R. Jones, S. Miglioranza, M. Pappagallo, and P. Robbe, The LHCb simulation application, Gauss: Design, evolution and experience, *J. Phys. Conf. Ser.* **331**, 032023 (2011).
- [29] I. Caprini, L. Lellouch, and M. Neubert, Dispersive bounds on the shape of $\bar{B} \rightarrow D^{(*)}$ lepton anti-neutrino form-factors, *Nucl. Phys.* **B530**, 153 (1998).
- [30] R. Aaij *et al.* (LHCb Collaboration), A precise measurement of the B^0 meson oscillation frequency, *Eur. Phys. J. C* **76**, 412 (2016).
- [31] P. A. Zyla *et al.* (Particle Data Group), Review of particle physics, *Prog. Theor. Exp. Phys.* **2020**, 083C01 (2020).
- [32] L. Breiman, J. H. Friedman, R. A. Olshen, and C. J. Stone, *Classification and Regression Trees* (Wadsworth international group, Belmont, California, USA, 1984).
- [33] R. E. Schapire and Y. Freund, A decision-theoretic generalization of on-line learning and an application to boosting, *J. Comput. Syst. Sci.* **55**, 119 (1997).
- [34] See Supplemental Material at <http://link.aps.org/supplemental/10.1103/PhysRevLett.128.191803> for the figure showing the distributions of the three main input variables to the BDT classifier, for signal and background, respectively; the figure showing the τ decay time distribution for low and high BDT output values; and the figure showing the $\Lambda_c^+\pi^-\pi^+\pi^-$ mass distribution in the normalization sample.
- [35] T. Aaltonen *et al.* (CDF Collaboration), Measurement of the branching fraction $\mathcal{B}(\Lambda_b^0 \rightarrow \Lambda_c^+\pi^-\pi^+\pi^-)$ at CDF, *Phys. Rev. D* **85**, 032003 (2012).
- [36] R. Aaij *et al.* (LHCb Collaboration), Measurements of the branching fractions for $B_{(s)}^0 \rightarrow D_{(s)}\pi\pi\pi$ and $\Lambda_b^0 \rightarrow \Lambda_c^+\pi\pi\pi$, *Phys. Rev. D* **84**, 092001 (2011); **85**, 039904(E) (2012).
- [37] J. Abdallah *et al.* (DELPHI Collaboration), Measurement of the Λ_b^0 decay form-factor, *Phys. Lett. B* **585**, 63 (2004).

- R. Aaij,³² A. S. W. Abdelmotteleb,⁵⁶ C. Abellán Beteta,⁵⁰ F. Abudinén,⁵⁶ T. Ackernley,⁶⁰ B. Adeva,⁴⁶ M. Adinolfi,⁵⁴ H. Afsharnia,⁹ C. Agapoulou,¹³ C. A. Aidala,⁸⁷ S. Aiola,²⁵ Z. Ajaltouni,⁹ S. Akar,⁶⁵ J. Albrecht,¹⁵ F. Alessio,⁴⁸ M. Alexander,⁵⁹ A. Alfonso Albero,⁴⁵ Z. Aliouche,⁶² G. Alkhazov,³⁸ P. Alvarez Cartelle,⁵⁵ S. Amato,² J. L. Amey,⁵⁴ Y. Amhis,¹¹ L. An,⁴⁸ L. Anderlini,²² M. Andersson,⁵⁰ A. Andreianov,³⁸ M. Andreotti,²¹ F. Archilli,¹⁷ A. Artamonov,⁴⁴ M. Artuso,⁶⁸ K. Arzimatov,⁴² E. Aslanides,¹⁰ M. Atzeni,⁵⁰ B. Audurier,¹² S. Bachmann,¹⁷ M. Bachmayer,⁴⁹ J. J. Back,⁵⁶ P. Baladron Rodriguez,⁴⁶ V. Balagura,¹² W. Baldini,²¹ J. Baptista de Souza Leite,¹ M. Barbetti,^{22,b} R. J. Barlow,⁶² S. Barsuk,¹¹ W. Barter,⁶¹ M. Bartolini,⁵⁵ F. Baryshnikov,⁸³ J. M. Basels,¹⁴ S. Bashir,³⁴ G. Bassi,²⁹ B. Batsukh,⁴ A. Battig,¹⁵ A. Bay,⁴⁹ A. Beck,⁵⁶ M. Becker,¹⁵ F. Bedeschi,²⁹ I. Bediaga,¹ A. Beiter,⁶⁸ V. Belavin,⁴² S. Belin,²⁷ V. Bellee,⁵⁰ K. Belous,⁴⁴ I. Belov,⁴⁰ I. Belyaev,⁴¹ G. Bencivenni,²³ E. Ben-Haim,¹³ A. Berezhnoy,⁴⁰ R. Bernet,⁵⁰ D. Berninghoff,¹⁷ H. C. Bernstein,⁶⁸ C. Bertella,⁶² A. Bertolin,²⁸ C. Betancourt,⁵⁰ F. Betti,⁴⁸ Ia. Bezshyiko,⁵⁰ S. Bhasin,⁵⁴ J. Bhom,³⁵ L. Bian,⁷³ M. S. Bieker,¹⁵ N. V. Biesuz,²¹ S. Bifani,⁵³ P. Billoir,¹³ A. Biolchini,³² M. Birch,⁶¹ F. C. R. Bishop,⁵⁵ A. Bitadze,⁶² A. Bizzeti,^{22,c} M. Bjørn,⁶³ M. P. Blago,⁵⁵ T. Blake,⁵⁶ F. Blanc,⁴⁹ S. Blusk,⁶⁸ D. Bobulska,⁵⁹ J. A. Boelhauve,¹⁵ O. Boente Garcia,⁴⁶ T. Boettcher,⁶⁵ A. Boldyrev,⁸² A. Bondar,⁴³ N. Bondar,^{38,48} S. Borghi,⁶² M. Borisjak,⁴² M. Borsato,¹⁷ J. T. Borsuk,³⁵ S. A. Bouchiba,⁴⁹ T. J. V. Bowcock,^{60,48} A. Boyer,⁴⁸ C. Bozzi,²¹ M. J. Bradley,⁶¹ S. Braun,⁶⁶ A. Brea Rodriguez,⁴⁶ J. Brodzicka,³⁵ A. Brossa Gonzalo,⁵⁶ D. Brundu,²⁷ A. Buonaura,⁵⁰ L. Buonincontri,²⁸ A. T. Burke,⁶² C. Burr,⁴⁸ A. Bursche,⁷² A. Butkevich,³⁹ J. S. Butter,³² J. Buytaert,⁴⁸ W. Byczynski,⁴⁸ S. Cadeddu,²⁷ H. Cai,⁷³ R. Calabrese,^{21,d} L. Calefice,^{15,13} S. Cali,²³ R. Calladine,⁵³ M. Calvi,^{26,e} M. Calvo Gomez,⁸⁵ P. Camargo Magalhaes,⁵⁴ P. Campana,²³ A. F. Campoverde Quezada,⁶ S. Capelli,^{26,e} L. Capriotti,^{20,f} A. Carbone,^{20,f} G. Carboni,^{31,g} R. Cardinale,^{24,h} A. Cardini,²⁷ I. Carli,⁴ P. Carniti,^{26,e} L. Carus,¹⁴ K. Carvalho Akiba,³² A. Casais Vidal,⁴⁶ R. Caspary,¹⁷ G. Casse,⁶⁰ M. Cattaneo,⁴⁸ G. Cavallero,⁴⁸ S. Celani,⁴⁹ J. Cerasoli,¹⁰ D. Cervenkov,⁶³ A. J. Chadwick,⁶⁰ M. G. Chapman,⁵⁴ M. Charles,¹³ Ph. Charpentier,⁴⁸ C. A. Chavez Barajas,⁶⁰ M. Chefdeville,⁸ C. Chen,³ S. Chen,⁴ A. Chernov,³⁵ V. Chobanova,⁴⁶ S. Cholak,⁴⁹ M. Chrzaszcz,³⁵ A. Chubykin,³⁸ V. Chulikov,³⁸ P. Ciambrone,²³ M. F. Cicala,⁵⁶ X. Cid Vidal,⁴⁶ G. Ciezarek,⁴⁸ P. E. L. Clarke,⁵⁸ M. Clemencic,⁴⁸ H. V. Cliff,⁵⁵ J. Closier,⁴⁸ J. L. Cobbledick,⁶² V. Coco,⁴⁸ J. A. B. Coelho,¹¹ J. Cogan,¹⁰ E. Cogneras,⁹ L. Cojocariu,³⁷ P. Collins,⁴⁸ T. Colombo,⁴⁸ L. Congedo,^{19,i} A. Contu,²⁷ N. Cooke,⁵³ G. Coombs,⁵⁹ I. Corredoira,⁴⁶ G. Corti,⁴⁸ C. M. Costa Sobral,⁵⁶ B. Couturier,⁴⁸ D. C. Craik,⁶⁴ J. Crkovská,⁶⁷ M. Cruz Torres,¹ R. Currie,⁵⁸ C. L. Da Silva,⁶⁷ S. Dadabaev,⁸³ L. Dai,⁷¹ E. Dall'Occo,¹⁵ J. Dalseno,⁴⁶ C. D'Ambrosio,⁴⁸ A. Danilina,⁴¹ P. d'Argent,⁴⁸ A. Dashkina,⁸³ J. E. Davies,⁶² A. Davis,⁶² O. De Aguiar Francisco,⁶² K. De Bruyn,⁷⁹ S. De Capua,⁶² M. De Cian,⁴⁹ U. De Freitas Carneiro Da Graca,¹ E. De Lucia,²³ J. M. De Miranda,¹ L. De Paula,² M. De Serio,^{19,i} D. De Simone,⁵⁰ P. De Simone,²³ F. De Vellis,¹⁵ J. A. de Vries,⁸⁰ C. T. Dean,⁶⁷ F. Debernardis,^{19,i} D. Decamp,⁸ V. Dedu,¹⁰ L. Del Buono,¹³ B. Delaney,⁵⁵ H.-P. Dembinski,¹⁵ V. Denysenko,⁵⁰ D. Derkach,⁸² O. Deschamps,⁹ F. Dettori,^{27,j} B. Dey,⁷⁷ A. Di Cicco,²³ P. Di Nezza,²³ S. Didenko,⁸³ L. Dieste Maronas,⁴⁶ H. Dijkstra,⁴⁸ V. Dobishuk,⁵² C. Dong,³ A. M. Donohoe,¹⁸ F. Dordei,²⁷ A. C. dos Reis,¹ L. Douglas,⁵⁹ A. Dovbnya,⁵¹ A. G. Downes,⁸ M. W. Dudek,³⁵ L. Dufour,⁴⁸ V. Duk,⁷⁸ P. Durante,⁴⁸ J. M. Durham,⁶⁷ D. Dutta,⁶² A. Dziurda,³⁵ A. Dzyuba,³⁸ S. Easo,⁵⁷ U. Egede,⁶⁹ V. Egorychev,⁴¹ S. Eidelman,^{43,a,k} S. Eisenhardt,⁵⁸ S. Ek-In,⁴⁹ L. Eklund,⁸⁶ S. Ely,⁶⁸ A. Ene,³⁷ E. Epple,⁶⁷ S. Escher,¹⁴ J. Eschle,⁵⁰ S. Esen,⁵⁰ T. Evans,⁶² L. N. Falcao,¹ Y. Fan,⁶ B. Fang,⁷³ S. Farry,⁶⁰ D. Fazzini,^{26,e} M. Féo,⁴⁸ A. Fernandez Prieto,⁴⁶ A. D. Fernez,⁶⁶ F. Ferrari,²⁰ L. Ferreira Lopes,⁴⁹ F. Ferreira Rodrigues,² S. Ferreres Sole,³² M. Ferrillo,⁵⁰ M. Ferro-Luzzi,⁴⁸ S. Filippov,³⁹ R. A. Fini,¹⁹ M. Fiorini,^{21,d} M. Firlej,³⁴ K. M. Fischer,⁶³ D. S. Fitzgerald,⁸⁷ C. Fitzpatrick,⁶² T. Fiutowski,³⁴ A. Fkiaras,⁴⁸ F. Fleuret,¹² M. Fontana,¹³ F. Fontanelli,^{24,h} R. Forty,⁴⁸ D. Foulds-Holt,⁵⁵ V. Franco Lima,⁶⁰ M. Franco Sevilla,⁶⁶ M. Frank,⁴⁸ E. Franzoso,²¹ G. Frau,¹⁷ C. Frei,⁴⁸ D. A. Friday,⁵⁹ J. Fu,⁶ Q. Fuehring,¹⁵ E. Gabriel,³² G. Galati,^{19,i} A. Gallas Torreira,⁴⁶ D. Galli,^{20,f} S. Gambetta,^{58,48} Y. Gan,³ M. Gandelman,² P. Gandini,²⁵ Y. Gao,⁵ M. Garau,²⁷ L. M. Garcia Martin,⁵⁶ P. Garcia Moreno,⁴⁵ J. Garcia Pardiñas,^{26,e} B. Garcia Plana,⁴⁶ F. A. Garcia Rosales,¹² L. Garrido,⁴⁵ C. Gaspar,⁴⁸ R. E. Geertsema,³² D. Gerick,¹⁷ L. L. Gerken,¹⁵ E. Gersabeck,⁶² M. Gersabeck,⁶² T. Gershon,⁵⁶ D. Gerstel,¹⁰ L. Giambastiani,²⁸ V. Gibson,⁵⁵ H. K. Giemza,³⁶ A. L. Gilman,⁶³ M. Giovannetti,^{23,g} A. Gioventù,⁴⁶ P. Gironella Gironell,⁴⁵ C. Giugliano,²¹ K. Gizdov,⁵⁸ E. L. Gkougkousis,⁴⁸ V. V. Gligorov,^{13,48} C. Göbel,⁷⁰ E. Golobardes,⁸⁵ D. Golubkov,⁴¹ A. Golutvin,^{61,83} A. Gomes,^{1,1} S. Gomez Fernandez,⁴⁵ F. Goncalves Abrantes,⁶³ M. Goncerz,³⁵ G. Gong,³ P. Gorbounov,⁴¹ I. V. Gorelov,⁴⁰ C. Gotti,²⁶ J. P. Grabowski,¹⁷ T. Grammatico,¹³ L. A. Granado Cardoso,⁴⁸ E. Graugés,⁴⁵ E. Graverini,⁴⁹

- G. Graziani,²² A. Grecu,³⁷ L. M. Greeven,³² N. A. Grieser,⁴ L. Grillo,⁶² S. Gromov,⁸³ B. R. Gruberg Cazon,⁶³ C. Gu,³ M. Guarise,²¹ M. Guittiere,¹¹ P. A. Günther,¹⁷ E. Gushchin,³⁹ A. Guth,¹⁴ Y. Guz,⁴⁴ T. Gys,⁴⁸ T. Hadavizadeh,⁶⁹ G. Haefeli,⁴⁹ C. Haen,⁴⁸ J. Haimberger,⁴⁸ S. C. Haines,⁵⁵ T. Halewood-leagas,⁶⁰ P. M. Hamilton,⁶⁶ J. P. Hammerich,⁶⁰ Q. Han,⁷ X. Han,¹⁷ E. B. Hansen,⁶² S. Hansmann-Menzemer,¹⁷ N. Harnew,⁶³ T. Harrison,⁶⁰ C. Hasse,⁴⁸ M. Hatch,⁴⁸ J. He,^{6,m} M. Hecker,⁶¹ K. Heijhoff,³² K. Heinicke,¹⁵ R. D. L. Henderson,^{69,56} A. M. Hennequin,⁴⁸ K. Hennessy,⁶⁰ L. Henry,⁴⁸ J. Heuel,¹⁴ A. Hicheur,² D. Hill,⁴⁹ M. Hilton,⁶² S. E. Hollitt,¹⁵ R. Hou,⁷ Y. Hou,⁸ J. Hu,¹⁷ J. Hu,⁷² W. Hu,⁷ X. Hu,³ W. Huang,⁶ X. Huang,⁷³ W. Hulsbergen,³² R. J. Hunter,⁵⁶ M. Hushchyn,⁸² D. Hutchcroft,⁶⁰ D. Hynds,³² P. Ibis,¹⁵ M. Idzik,³⁴ D. Ilin,³⁸ P. Ilten,⁶⁵ A. Inglessi,³⁸ A. Ishteev,⁸³ K. Ivshin,³⁸ R. Jacobsson,⁴⁸ H. Jage,¹⁴ S. Jakobsen,⁴⁸ E. Jans,³² B. K. Jashal,⁴⁷ A. Jawahery,⁶⁶ V. Jevtic,¹⁵ X. Jiang,⁴ M. John,⁶³ D. Johnson,⁶⁴ C. R. Jones,⁵⁵ T. P. Jones,⁵⁶ B. Jost,⁴⁸ N. Jurik,⁴⁸ S. H. Kalavan Kadavath,³⁴ S. Kandybei,⁵¹ Y. Kang,³ M. Karacson,⁴⁸ D. Karpenkov,⁸³ M. Karpov,⁸² J. W. Kautz,⁶⁵ F. Keizer,⁴⁸ D. M. Keller,⁶⁸ M. Kenzie,⁵⁶ T. Ketel,³³ B. Khanji,¹⁵ A. Kharisova,⁸⁴ S. Kholodenko,⁴⁴ T. Kirn,¹⁴ V. S. Kirsebom,⁴⁹ O. Kitouni,⁶⁴ S. Klaver,³³ N. Kleijne,²⁹ K. Klimaszewski,³⁶ M. R. Kmiec,³⁶ S. Kolliiev,⁵² A. Kondybayeva,⁸³ A. Konoplyannikov,⁴¹ P. Kopciewicz,³⁴ R. Kopecna,¹⁷ P. Koppenburg,³² M. Korolev,⁴⁰ I. Kostiuk,^{32,52} O. Kot,⁵² S. Kotriakhova,^{21,38} A. Kozachuk,⁴⁰ P. Kravchenko,³⁸ L. Kravchuk,³⁹ R. D. Krawczyk,⁴⁸ M. Kreps,⁵⁶ S. Kretzschmar,¹⁴ P. Krokovny,^{43,k} W. Krupa,³⁴ W. Krzemien,³⁶ J. Kubat,¹⁷ M. Kucharczyk,³⁵ V. Kudryavtsev,^{43,k} H. S. Kuindersma,^{32,33} G. J. Kunde,⁶⁷ T. Kvaratskheliya,⁴¹ D. Lacarrere,⁴⁸ G. Lafferty,⁶² A. Lai,²⁷ A. Lampis,²⁷ D. Lancierini,⁵⁰ J. J. Lane,⁶² R. Lane,⁵⁴ G. Lanfranchi,²³ C. Langenbruch,¹⁴ J. Langer,¹⁵ O. Lantwin,⁸³ T. Latham,⁵⁶ F. Lazzari,²⁹ R. Le Gac,¹⁰ S. H. Lee,⁸⁷ R. Lefèvre,⁹ A. Leflat,⁴⁰ S. Legotin,⁸³ O. Leroy,¹⁰ T. Lesiak,³⁵ B. Leverington,¹⁷ H. Li,⁷² P. Li,¹⁷ S. Li,⁷ Y. Li,⁴ Z. Li,⁶⁸ X. Liang,⁶⁸ T. Lin,⁶¹ R. Lindner,⁴⁸ V. Lisovskyi,¹⁵ R. Litvinov,²⁷ G. Liu,⁷² H. Liu,⁶ Q. Liu,⁶ S. Liu,⁴ A. Lobo Salvia,⁴⁵ A. Loi,²⁷ R. Lollini,⁷⁸ J. Lomba Castro,⁴⁶ I. Longstaff,⁵⁹ J. H. Lopes,² S. López Soliño,⁴⁶ G. H. Lovell,⁵⁵ Y. Lu,⁴ C. Lucarelli,^{22,b} D. Lucchesi,^{28,n} S. Luchuk,³⁹ M. Lucio Martinez,³² V. Lukashenko,^{32,52} Y. Luo,³ A. Lupato,⁶² E. Luppi,^{21,d} O. Lupton,⁵⁶ A. Lusiani,^{29,o} X. Lyu,⁶ L. Ma,⁴ R. Ma,⁶ S. Maccolini,²⁰ F. Machefert,¹¹ F. Maciuc,³⁷ V. Macko,⁴⁹ P. Mackowiak,¹⁵ S. Maddrell-Mander,⁵⁴ O. Madejczyk,³⁴ L. R. Madhan Mohan,⁵⁴ O. Maev,³⁸ A. Maevskiy,⁸² D. Maisuzenko,³⁸ M. W. Majewski,³⁴ J. J. Malczewski,³⁵ S. Malde,⁶³ B. Malecki,³⁵ A. Malinin,⁸¹ T. Maltsev,^{43,k} H. Malygina,¹⁷ G. Manca,^{27,j} G. Mancinelli,¹⁰ D. Manuzzi,²⁰ D. Marangotto,^{25,p} J. Maratas,^{9,q} J. F. Marchand,⁸ U. Marconi,²⁰ S. Mariani,^{22,b} C. Marin Benito,⁴⁸ M. Marinangeli,⁴⁹ J. Marks,¹⁷ A. M. Marshall,⁵⁴ P. J. Marshall,⁶⁰ G. Martelli,⁷⁸ G. Martellotti,³⁰ L. Martinazzoli,^{48,e} M. Martinelli,^{26,e} D. Martinez Santos,⁴⁶ F. Martinez Vidal,⁴⁷ A. Massafferri,¹ M. Materok,¹⁴ R. Matev,⁴⁸ A. Mathad,⁵⁰ V. Matiunin,⁴¹ C. Matteuzzi,²⁶ K. R. Mattioli,⁸⁷ A. Mauri,³² E. Maurice,¹² J. Mauricio,⁴⁵ M. Mazurek,⁴⁸ M. McCann,⁶¹ L. McConnell,¹⁸ T. H. McGrath,⁶² N. T. Mchugh,⁵⁹ A. McNab,⁶² R. McNulty,¹⁸ J. V. Mead,⁶⁰ B. Meadows,⁶⁵ G. Meier,¹⁵ D. Melnychuk,³⁶ S. Meloni,^{26,e} M. Merk,^{32,80} A. Merli,^{25,p} L. Meyer Garcia,² M. Mikhasenko,^{75,r} D. A. Milanes,⁷⁴ E. Millard,⁵⁶ M. Milovanovic,⁴⁸ M.-N. Minard,⁸ A. Minotti,^{26,e} S. E. Mitchell,⁵⁸ B. Mitreska,⁶² D. S. Mitzel,¹⁵ A. Mödden,¹⁵ R. A. Mohammed,⁶³ R. D. Moise,⁶¹ S. Mokhnenko,⁸² T. Mombächer,⁴⁶ I. A. Monroy,⁷⁴ S. Monteil,⁹ M. Morandin,²⁸ G. Morello,²³ M. J. Morello,^{29,o} J. Moron,³⁴ A. B. Morris,⁷⁵ A. G. Morris,⁵⁶ R. Mountain,⁶⁸ H. Mu,³ F. Muheim,⁵⁸ M. Mulder,⁷⁹ K. Müller,⁵⁰ C. H. Murphy,⁶³ D. Murray,⁶² R. Murta,⁶¹ P. Muzzetto,²⁷ P. Naik,⁵⁴ T. Nakada,⁴⁹ R. Nandakumar,⁵⁷ T. Nanut,⁴⁸ I. Nasteva,² M. Needham,⁵⁸ N. Neri,^{25,p} S. Neubert,⁷⁵ N. Neufeld,⁴⁸ R. Newcombe,⁶¹ E. M. Niel,⁴⁹ S. Nieswand,¹⁴ N. Nikitin,⁴⁰ N. S. Nolte,⁶⁴ C. Normand,⁸ C. Nunez,⁸⁷ A. Oblakowska-Mucha,³⁴ V. Obraztsov,⁴⁴ T. Oeser,¹⁴ D. P. O'Hanlon,⁵⁴ S. Okamura,²¹ R. Oldeman,^{27,j} F. Oliva,⁵⁸ M. E. Olivares,⁶⁸ C. J. G. Onderwater,⁷⁹ R. H. O'Neil,⁵⁸ J. M. Otalora Goicochea,² T. Ovsiannikova,⁴¹ P. Owen,⁵⁰ A. Oyanguren,⁴⁷ O. Ozcelik,⁵⁸ K. O. Padeken,⁷⁵ B. Pagare,⁵⁶ P. R. Pais,⁴⁸ T. Pajero,⁶³ A. Palano,¹⁹ M. Palutan,²³ Y. Pan,⁶² G. Panshin,⁸⁴ A. Papanestis,⁵⁷ M. Pappagallo,^{19,i} L. L. Pappalardo,^{21,d} C. Pappenheimer,⁶⁵ W. Parker,⁶⁶ C. Parkes,⁶² B. Passalacqua,²¹ G. Passaleva,²² A. Pastore,¹⁹ M. Patel,⁶¹ C. Patrignani,^{20,f} C. J. Pawley,⁸⁰ A. Pearce,^{48,57} A. Pellegrino,³² M. Pepe Altarelli,⁴⁸ S. Perazzini,²⁰ D. Pereima,⁴¹ A. Pereiro Castro,⁴⁶ P. Perret,⁹ M. Petric,^{59,48} K. Petridis,⁵⁴ A. Petrolini,^{24,h} A. Petrov,⁸¹ S. Petrucci,⁵⁸ M. Petruzzo,²⁵ T. T. H. Pham,⁶⁸ A. Philippov,⁴² R. Piandani,⁶ L. Pica,^{29,o} M. Piccini,⁷⁸ B. Pietrzyk,⁸ G. Pietrzyk,¹¹ M. Pili,⁶³ D. Pinci,³⁰ F. Pisani,⁴⁸ M. Pizzichemi,^{26,48,e} P. K. Resmi,¹⁰ V. Placinta,³⁷ J. Plews,⁵³ M. Plo Casasus,⁴⁶ F. Polci,^{13,48} M. Poli Lener,²³ M. Poliakova,⁶⁸ A. Poluektov,¹⁰ N. Polukhina,^{83,s} I. Polyakov,⁶⁸ E. Polycarpo,² S. Ponce,⁴⁸ D. Popov,^{6,48} S. Popov,⁴² S. Poslavskii,⁴⁴ K. Prasanth,³⁵ L. Promberger,⁴⁸ C. Prouve,⁴⁶ V. Pugatch,⁵² V. Puill,¹¹ G. Punzi,^{29,t} H. Qi,³ W. Qian,⁶ N. Qin,³ R. Quagliani,⁴⁹ N. V. Raab,¹⁸ R. I. Rabadan Trejo,⁶ B. Rachwal,³⁴ J. H. Rademacker,⁵⁴ R. Rajagopalan,⁶⁸ M. Rama,²⁹ M. Ramos Pernas,⁵⁶ M. S. Rangel,² F. Ratnikov,^{42,82} G. Raven,^{33,48} M. Reboud,⁸ F. Redi,⁴⁸ F. Reiss,⁶² C. Remon Alepuz,⁴⁷ Z. Ren,³ V. Renaudin,⁶³ R. Ribatti,²⁹ A. M. Ricci,²⁷

S. Ricciardi,⁵⁷ K. Rinnert,⁶⁰ P. Robbe,¹¹ G. Robertson,⁵⁸ A. B. Rodrigues,⁴⁹ E. Rodrigues,⁶⁰ J. A. Rodriguez Lopez,⁷⁴ E. R. R. Rodriguez Rodriguez,⁴⁶ A. Rollings,⁶³ P. Roloff,⁴⁸ V. Romanovskiy,⁴⁴ M. Romero Lamas,⁴⁶ A. Romero Vidal,⁴⁶ J. D. Roth,⁸⁷ M. Rotondo,²³ M. S. Rudolph,⁶⁸ T. Ruf,⁴⁸ R. A. Ruiz Fernandez,⁴⁶ J. Ruiz Vidal,⁴⁷ A. Ryzhikov,⁸² J. Ryzka,³⁴ J. J. Saborido Silva,⁴⁶ N. Sagidova,³⁸ N. Sahoo,⁵³ B. Saitta,^{27,j} M. Salomoni,⁴⁸ C. Sanchez Gras,³² R. Santacesaria,³⁰ C. Santamarina Rios,⁴⁶ M. Santimaria,²³ E. Santovetti,^{31,g} D. Saranin,⁸³ G. Sarpis,¹⁴ M. Sarpis,⁷⁵ A. Sarti,³⁰ C. Satriano,^{30,u} A. Satta,³¹ M. Saur,¹⁵ D. Savrina,^{41,40} H. Sazak,⁹ L. G. Scantlebury Smead,⁶³ A. Scarabotto,¹³ S. Schael,¹⁴ S. Scherl,⁶⁰ M. Schiller,⁵⁹ H. Schindler,⁴⁸ M. Schmelling,¹⁶ B. Schmidt,⁴⁸ S. Schmitt,¹⁴ O. Schneider,⁴⁹ A. Schopper,⁴⁸ M. Schubiger,³² S. Schulte,⁴⁹ M. H. Schune,¹¹ R. Schwemmer,⁴⁸ B. Sciascia,^{23,48} S. Sellam,⁴⁶ A. Semennikov,⁴¹ M. Senghi Soares,³³ A. Sergi,^{24,h} N. Serra,⁵⁰ L. Sestini,²⁸ A. Seuthe,¹⁵ Y. Shang,⁵ D. M. Shangase,⁸⁷ M. Shapkin,⁴⁴ I. Shchemerov,⁸³ L. Shchutska,⁴⁹ T. Shears,⁶⁰ L. Shekhtman,^{43,k} Z. Shen,⁵ S. Sheng,⁴ V. Shevchenko,⁸¹ E. B. Shields,^{26,e} Y. Shimizu,¹¹ E. Shmanin,⁸³ J. D. Shupperd,⁶⁸ B. G. Siddi,²¹ R. Silva Coutinho,⁵⁰ G. Simi,²⁸ S. Simone,^{19,i} N. Skidmore,⁶² R. Skuza,¹⁷ T. Skwarnicki,⁶⁸ M. W. Slater,⁵³ I. Slazyk,^{21,d} J. C. Smallwood,⁶³ J. G. Smeaton,⁵⁵ E. Smith,⁵⁰ M. Smith,⁶¹ A. Snoch,³² L. Soares Lavra,⁹ M. D. Sokoloff,⁶⁵ F. J. P. Soler,⁵⁹ A. Solovev,³⁸ I. Solovyev,³⁸ F. L. Souza De Almeida,² B. Souza De Paula,² B. Spaan,¹⁵ E. Spadaro Norella,^{25,p} P. Spradlin,⁵⁹ F. Stagni,⁴⁸ M. Stahl,⁶⁵ S. Stahl,⁴⁸ S. Stanislaus,⁶³ O. Steinkamp,^{50,83} O. Stenyakin,⁴⁴ H. Stevens,¹⁵ S. Stone,^{68,48,a} D. Strekalina,⁸³ F. Suljik,⁶³ J. Sun,²⁷ L. Sun,⁷³ Y. Sun,⁶⁶ P. Svihre,⁶² P. N. Swallow,⁵³ K. Swientek,³⁴ A. Szabelski,³⁶ T. Szumlak,³⁴ M. Szymanski,⁴⁸ S. Taneja,⁶² A. R. Tanner,⁵⁴ M. D. Tat,⁶³ A. Terentev,⁸³ F. Teubert,⁴⁸ E. Thomas,⁴⁸ D. J. D. Thompson,⁵³ K. A. Thomson,⁶⁰ H. Tilquin,⁶¹ V. Tisserand,⁹ S. T'Jampens,⁸ M. Tobin,⁴ L. Tomassetti,^{21,d} X. Tong,⁵ D. Torres Machado,¹ D. Y. Tou,³ E. Trifonova,⁸³ S. M. Trilov,⁵⁴ C. Tripli,⁴⁹ G. Tuci,⁶ A. Tully,⁴⁹ N. Tuning,^{32,48} A. Ukleja,^{36,48} D. J. Unverzagt,¹⁷ E. Ursov,⁸³ A. Usachov,³² A. Ustyuzhanin,^{42,82} U. Uwer,¹⁷ A. Vagner,⁸⁴ V. Vagnoni,²⁰ A. Valassi,⁴⁸ G. Valenti,²⁰ N. Valls Canudas,⁸⁵ M. van Beuzekom,³² M. Van Dijk,⁴⁹ H. Van Hecke,⁶⁷ E. van Herwijnen,⁸³ M. van Veghel,⁷⁹ R. Vazquez Gomez,⁴⁵ P. Vazquez Regueiro,⁴⁶ C. Vázquez Sierra,⁴⁸ S. Vecchi,²¹ J. J. Velthuis,⁵⁴ M. Veltri,^{22,v} A. Venkateswaran,⁶⁸ M. Veronesi,³² M. Vesterinen,⁵⁶ D. Vieira,⁶⁵ M. Vieites Diaz,⁴⁹ H. Viemann,⁷⁶ X. Vilasis-Cardona,⁸⁵ E. Vilella Figueras,⁶⁰ A. Villa,²⁰ P. Vincent,¹³ F. C. Volle,¹¹ D. Vom Bruch,¹⁰ A. Vorobyev,³⁸ V. Vorobyev,^{43,k} N. Voropaev,³⁸ K. Vos,⁸⁰ R. Waldi,¹⁷ J. Walsh,²⁹ C. Wang,¹⁷ J. Wang,⁵ J. Wang,⁴ J. Wang,³ J. Wang,⁷³ M. Wang,³ R. Wang,⁵⁴ Y. Wang,⁷ Z. Wang,⁵⁰ Z. Wang,³ Z. Wang,⁶ J. A. Ward,^{56,69} N. K. Watson,⁵³ D. Websdale,⁶¹ C. Weisser,⁶⁴ B. D. C. Westhenry,⁵⁴ D. J. White,⁶² M. Whitehead,⁵⁴ A. R. Wiederhold,⁵⁶ D. Wiedner,¹⁵ G. Wilkinson,⁶³ M. K. Wilkinson,⁶⁸ I. Williams,⁵⁵ M. Williams,⁶⁴ M. R. J. Williams,⁵⁸ F. F. Wilson,⁵⁷ W. Wislicki,³⁶ M. Wittek,³⁵ L. Witola,¹⁷ G. Wormser,¹¹ S. A. Wotton,⁵⁵ H. Wu,⁶⁸ K. Wyllie,⁴⁸ Z. Xiang,⁶ D. Xiao,⁷ Y. Xie,⁷ A. Xu,⁵ J. Xu,⁶ L. Xu,³ M. Xu,⁵⁶ Q. Xu,⁶ Z. Xu,⁹ Z. Xu,⁶ D. Yang,³ S. Yang,⁶ Y. Yang,⁶ Z. Yang,⁵ Z. Yang,⁶⁶ Y. Yao,⁶⁸ L. E. Yeomans,⁶⁰ H. Yin,⁷ J. Yu,⁷¹ X. Yuan,⁶⁸ O. Yushchenko,⁴⁴ E. Zaffaroni,⁴⁹ M. Zavertyaev,^{16,s} M. Zdybal,³⁵ O. Zenaiev,⁴⁸ M. Zeng,³ D. Zhang,⁷ L. Zhang,³ S. Zhang,⁷¹ S. Zhang,⁵ Y. Zhang,⁵ Y. Zhang,⁶³ A. Zharkova,⁸³ A. Zhelezov,¹⁷ Y. Zheng,⁶ T. Zhou,⁵ X. Zhou,⁶ Y. Zhou,⁶ V. Zhovkovska,¹¹ X. Zhu,³ X. Zhu,⁷ Z. Zhu,⁶ V. Zhukov,^{14,40} Q. Zou,⁴ S. Zucchelli,^{20,f} D. Zuliani,²⁸ and G. Zunica⁶²

(LHCb Collaboration)

¹Centro Brasileiro de Pesquisas Físicas (CBPF), Rio de Janeiro, Brazil²Universidade Federal do Rio de Janeiro (UFRJ), Rio de Janeiro, Brazil³Center for High Energy Physics, Tsinghua University, Beijing, China⁴Institute Of High Energy Physics (IHEP), Beijing, China⁵School of Physics State Key Laboratory of Nuclear Physics and Technology, Peking University, Beijing, China⁶University of Chinese Academy of Sciences, Beijing, China⁷Institute of Particle Physics, Central China Normal University, Wuhan, Hubei, China⁸Université Savoie Mont Blanc, CNRS, IN2P3-LAPP, Annecy, France⁹Université Clermont Auvergne, CNRS/IN2P3, LPC, Clermont-Ferrand, France¹⁰Aix Marseille Université, CNRS/IN2P3, CPPM, Marseille, France¹¹Université Paris-Saclay, CNRS/IN2P3, IJCLab, Orsay, France¹²Laboratoire Leprince-Ringuet, CNRS/IN2P3, Ecole Polytechnique, Institut Polytechnique de Paris, Palaiseau, France¹³LPNHE, Sorbonne Université, Paris Diderot Sorbonne Paris Cité, CNRS/IN2P3, Paris, France¹⁴I. Physikalisches Institut, RWTH Aachen University, Aachen, Germany¹⁵Fakultät Physik, Technische Universität Dortmund, Dortmund, Germany

- ¹⁶Max-Planck-Institut für Kernphysik (MPIK), Heidelberg, Germany
¹⁷Physikalisches Institut, Ruprecht-Karls-Universität Heidelberg, Heidelberg, Germany
¹⁸School of Physics, University College Dublin, Dublin, Ireland
¹⁹INFN Sezione di Bari, Bari, Italy
²⁰INFN Sezione di Bologna, Bologna, Italy
²¹INFN Sezione di Ferrara, Ferrara, Italy
²²INFN Sezione di Firenze, Firenze, Italy
²³INFN Laboratori Nazionali di Frascati, Frascati, Italy
²⁴INFN Sezione di Genova, Genova, Italy
²⁵INFN Sezione di Milano, Milano, Italy
²⁶INFN Sezione di Milano-Bicocca, Milano, Italy
²⁷INFN Sezione di Cagliari, Monserrato, Italy
²⁸Università degli Studi di Padova, Università e INFN, Padova, Padova, Italy
²⁹INFN Sezione di Pisa, Pisa, Italy
³⁰INFN Sezione di Roma La Sapienza, Roma, Italy
³¹INFN Sezione di Roma Tor Vergata, Roma, Italy
³²Nikhef National Institute for Subatomic Physics, Amsterdam, Netherlands
³³Nikhef National Institute for Subatomic Physics and VU University Amsterdam, Amsterdam, Netherlands
³⁴AGH - University of Science and Technology, Faculty of Physics and Applied Computer Science, Kraków, Poland
³⁵Henryk Niewodniczanski Institute of Nuclear Physics Polish Academy of Sciences, Kraków, Poland
³⁶National Center for Nuclear Research (NCBJ), Warsaw, Poland
³⁷Horia Hulubei National Institute of Physics and Nuclear Engineering, Bucharest-Magurele, Romania
³⁸Petersburg Nuclear Physics Institute NRC Kurchatov Institute (PNPI NRC KI), Gatchina, Russia
³⁹Institute for Nuclear Research of the Russian Academy of Sciences (INR RAS), Moscow, Russia
⁴⁰Institute of Nuclear Physics, Moscow State University (SINP MSU), Moscow, Russia
⁴¹Institute of Theoretical and Experimental Physics NRC Kurchatov Institute (ITEP NRC KI), Moscow, Russia
⁴²Yandex School of Data Analysis, Moscow, Russia
⁴³Budker Institute of Nuclear Physics (SB RAS), Novosibirsk, Russia
⁴⁴Institute for High Energy Physics NRC Kurchatov Institute (IHEP NRC KI), Protvino, Russia, Protvino, Russia
⁴⁵ICCUB, Universitat de Barcelona, Barcelona, Spain
⁴⁶Instituto Galego de Física de Altas Enerxías (IGFAE), Universidade de Santiago de Compostela, Santiago de Compostela, Spain
⁴⁷Instituto de Física Corpuscular, Centro Mixto Universidad de Valencia - CSIC, Valencia, Spain
⁴⁸European Organization for Nuclear Research (CERN), Geneva, Switzerland
⁴⁹Institute of Physics, Ecole Polytechnique Fédérale de Lausanne (EPFL), Lausanne, Switzerland
⁵⁰Physik-Institut, Universität Zürich, Zürich, Switzerland
⁵¹NSC Kharkiv Institute of Physics and Technology (NSC KIPT), Kharkiv, Ukraine
⁵²Institute for Nuclear Research of the National Academy of Sciences (KINR), Kyiv, Ukraine
⁵³University of Birmingham, Birmingham, United Kingdom
⁵⁴H.H. Wills Physics Laboratory, University of Bristol, Bristol, United Kingdom
⁵⁵Cavendish Laboratory, University of Cambridge, Cambridge, United Kingdom
⁵⁶Department of Physics, University of Warwick, Coventry, United Kingdom
⁵⁷STFC Rutherford Appleton Laboratory, Didcot, United Kingdom
⁵⁸School of Physics and Astronomy, University of Edinburgh, Edinburgh, United Kingdom
⁵⁹School of Physics and Astronomy, University of Glasgow, Glasgow, United Kingdom
⁶⁰Oliver Lodge Laboratory, University of Liverpool, Liverpool, United Kingdom
⁶¹Imperial College London, London, United Kingdom
⁶²Department of Physics and Astronomy, University of Manchester, Manchester, United Kingdom
⁶³Department of Physics, University of Oxford, Oxford, United Kingdom
⁶⁴Massachusetts Institute of Technology, Cambridge, Massachusetts, USA
⁶⁵University of Cincinnati, Cincinnati, Ohio, USA
⁶⁶University of Maryland, College Park, Maryland, USA
⁶⁷Los Alamos National Laboratory (LANL), Los Alamos, New Mexico, USA
⁶⁸Syracuse University, Syracuse, New York, USA
⁶⁹School of Physics and Astronomy, Monash University, Melbourne, Australia
(associated with Department of Physics, University of Warwick, Coventry, United Kingdom)
⁷⁰Pontifícia Universidade Católica do Rio de Janeiro (PUC-Rio), Rio de Janeiro, Brazil
(associated with Universidade Federal do Rio de Janeiro (UFRJ), Rio de Janeiro, Brazil)
⁷¹Physics and Micro Electronic College, Hunan University, Changsha City, China
(associated with Institute of Particle Physics, Central China Normal University, Wuhan, Hubei, China)

- ⁷²Guangdong Provincial Key Laboratory of Nuclear Science, Guangdong-Hong Kong Joint Laboratory of Quantum Matter,
 Institute of Quantum Matter, South China Normal University, Guangzhou, China
 (associated with Center for High Energy Physics, Tsinghua University, Beijing, China)
- ⁷³School of Physics and Technology, Wuhan University, Wuhan, China
 (associated with Center for High Energy Physics, Tsinghua University, Beijing, China)
- ⁷⁴Departamento de Fisica, Universidad Nacional de Colombia, Bogota, Colombia
 (associated with LPNHE, Sorbonne Université, Paris Diderot Sorbonne Paris Cité, CNRS/IN2P3, Paris, France)
- ⁷⁵Universität Bonn - Helmholtz-Institut für Strahlen und Kernphysik, Bonn, Germany
 (associated with Physikalisches Institut, Ruprecht-Karls-Universität Heidelberg, Heidelberg, Germany)
- ⁷⁶Institut für Physik, Universität Rostock, Rostock, Germany
 (associated with Physikalisches Institut, Ruprecht-Karls-Universität Heidelberg, Heidelberg, Germany)
- ⁷⁷Eotvos Lorand University, Budapest, Hungary
 (associated with European Organization for Nuclear Research (CERN), Geneva, Switzerland)
- ⁷⁸INFN Sezione di Perugia, Perugia, Italy
 (associated with INFN Sezione di Ferrara, Ferrara, Italy)
- ⁷⁹Van Swinderen Institute, University of Groningen, Groningen, Netherlands
 (associated with Nikhef National Institute for Subatomic Physics, Amsterdam, Netherlands)
- ⁸⁰Universiteit Maastricht, Maastricht, Netherlands
 (associated with Nikhef National Institute for Subatomic Physics, Amsterdam, Netherlands)
- ⁸¹National Research Centre Kurchatov Institute, Moscow, Russia
 (associated with Institute of Theoretical and Experimental Physics NRC Kurchatov Institute (ITEP NRC KI), Moscow, Russia)
- ⁸²National Research University Higher School of Economics, Moscow, Russia
 (associated with Yandex School of Data Analysis, Moscow, Russia)
- ⁸³National University of Science and Technology “MISIS”, Moscow, Russia
 (associated with Institute of Theoretical and Experimental Physics NRC Kurchatov Institute (ITEP NRC KI), Moscow, Russia)
- ⁸⁴National Research Tomsk Polytechnic University, Tomsk, Russia
 (associated with Institute of Theoretical and Experimental Physics NRC Kurchatov Institute (ITEP NRC KI), Moscow, Russia)
- ⁸⁵DS4DS, La Salle, Universitat Ramon Llull, Barcelona, Spain
 (associated with ICCUB, Universitat de Barcelona, Barcelona, Spain)
- ⁸⁶Department of Physics and Astronomy, Uppsala University, Uppsala, Sweden
 (associated with School of Physics and Astronomy, University of Glasgow, Glasgow, United Kingdom)
- ⁸⁷University of Michigan, Michigan, Ann Arbor, USA
 (associated with Syracuse University, Syracuse, New York, USA)

^aDeceased.^bAlso at Università di Firenze, Firenze, Italy.^cAlso at Università di Modena e Reggio Emilia, Modena, Italy.^dAlso at Università di Ferrara, Ferrara, Italy.^eAlso at Università di Milano Bicocca, Milano, Italy.^fAlso at Università di Bologna, Bologna, Italy.^gAlso at Università di Roma Tor Vergata, Roma, Italy.^hAlso at Università di Genova, Genova, Italy.ⁱAlso at Università di Bari, Bari, Italy.^jAlso at Università di Cagliari, Cagliari, Italy.^kAlso at Novosibirsk State University, Novosibirsk, Russia.^lAlso at Universidade Federal do Triângulo Mineiro (UFTM), Uberaba-MG, Brazil.^mAlso at Hangzhou Institute for Advanced Study, UCAS, Hangzhou, China.ⁿAlso at Università di Padova, Padova, Italy.^oAlso at Scuola Normale Superiore, Pisa, Italy.^pAlso at Università degli Studi di Milano, Milano, Italy.^qAlso at MSU—Iligan Institute of Technology (MSU-IIT), Iligan, Philippines.^rAlso at Excellence Cluster ORIGINS, Munich, Germany.^sAlso at P.N. Lebedev Physical Institute, Russian Academy of Science (LPI RAS), Moscow, Russia.^tAlso at Università di Pisa, Pisa, Italy.^uAlso at Università della Basilicata, Potenza, Italy.^vAlso at Università di Urbino, Urbino, Italy.